Extreme wave run-up on a vertical cliff

Francesco Carbone[1], Denys Dutykh[1], John M. Dudley[2], Frédéric Dias[1]

[1] *School of Mathematical Sciences, University College of Dublin, Ireland,*

[3] *Institut FEMTO-ST, UMR 6174 CNRS-Université de Franche-Comté, Besançon, France*

The notion of *design wave* is usually used by engineers to dimension various coastal structures[7], even if there is a difficulty in determining the wave height to be used in semi-empirical formulas for the pressure field. In general, by considering an idealized simple monochromatic wave component with amplitude a_0, its wave height can be trivially computed to be $H_0 \sim 2a_0$, and consequently the design wave. Here we show that even a simple monochromatic sea state, subject to nonlinear dynamics on the flat bottom, can produce much higher amplitudes on a vertical wall. This suggests that the concept of design wave has to be revisited. Moreover, recalling that 89% of reported past freak wave events happened in shallow waters or coastal areas[9], our work can shed some light onto the extreme wave events in the shallow water regime.

One of the most important questions in water wave theory is the understanding of wave interaction and reflection. We describe the wave propagation of the free surface of an incompressible homogeneous inviscid fluid, through the fully nonlinear Serre–Green–Naghdi (SGN) equations[8,12]. We consider a two-dimensional wave tank with a flat impermeable bottom of uniform depth $d = $ const, which is filled with an incompressible, inviscid fluid. The Cartesian coordinate system Oxy is chosen such that the axis Oy points vertically upwards and the horizontal axis Ox coincides with the undisturbed water level $y = 0$.

The SGN system reads[2,4]:

$$h_t + (hu)_x = 0, \tag{1}$$

$$u_t + \left(\tfrac{1}{2}u^2 + gh\right)_x = \tfrac{1}{3}h^{-1}\left[h^3\left(u_{xt} + uu_{xx} - u_x^2\right)\right]_x, \tag{2}$$

where $h(x,t) := d + \eta(x,t)$ is the total water depth ($\eta(x,t)$ being the free surface elevation with respect to the water level), while $u(x,t)$ is the depth-averaged horizontal velocity, g is the gravity acceleration. The model has been previously validated by extensive comparisons with experimental data for wave propagation and run-up[5].

In our numerical experiments we consider a flat channel of length ℓ, bounded on the right by a rigid vertical wall and by a wavemaker on the left. Hereinbelow we will use the dimensionless variables in which all the lengths are normalized with d, speeds with $\sqrt{gd}$ and time with $\sqrt{d/g}$. This scaling is equivalent to setting $g = 1$ m/s², $d = 1$ m in the governing equations (1), (2).

In order to solve numerically the SGN equations we use a high-order finite-volume scheme[5], while for time integration we use the fourth-order Runge–Kutta scheme. The computational domain is divided into equal intervals (i.e. control volumes) such that we have $N = 1000$ control volumes per wavelength. The initial conditions are the state of rest $\eta(x, t = 0) \equiv 0$, $u(x, t = 0) \equiv 0$. On the wavemaker we generate a monochromatic incident wave $\eta(x = 0, t) = \eta_0(t) = a_0 \sin(\omega t)\mathcal{H}(T - t)$, where T represent the final generation time and the amplitude is fixed to the value $a_0 = 0.05$, $\omega \in [0.01, 0.25]$, and $\mathcal{H}(t)$ is the Heaviside function. We generate only a finite number N_w of waves with period $T_0 = 2\pi/\omega$, say $T := N_w T_0$. The length ℓ of the computational domain and the final simulation time T_f are
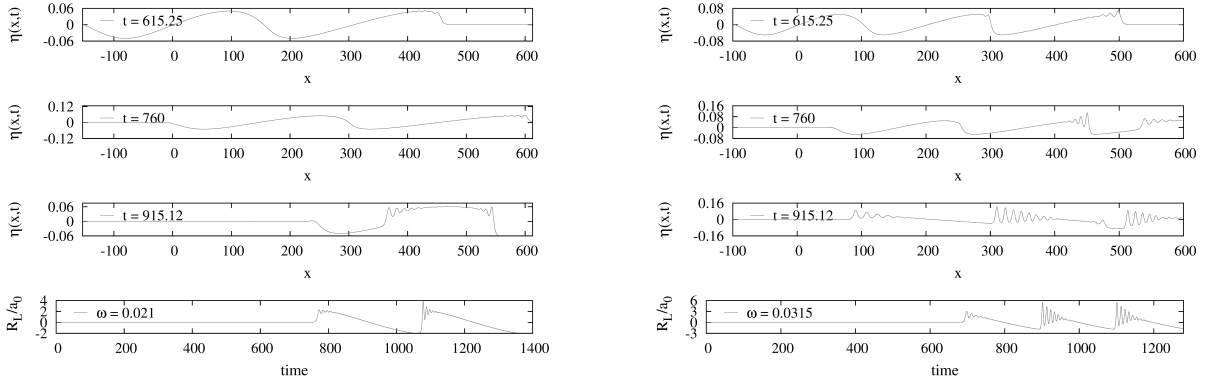
FIG. 1. Time evolution of the free surface elevation as a function of space, at three different times, left column two-wave case, right column three-wave case. The lower panel reports the maximal elevation at the wall $\mathcal{R}_\ell/a_0$ as a function of time.

chosen adaptively in order to allow all important interactions and to prevent any kind of reflections with the left generating boundary:

$$\ell = (N_w + \tfrac{1}{2})\lambda_0, \quad T_f = \frac{\ell}{\sqrt{g(d + a_0)}} + T, \tag{3}$$

λ_0 being the wavelength corresponding to the frequency ω.

We begin our experiments by considering a single sinusoidal wave interacting with the solid wall. The maximal wave elevation $\mathcal{R}_{\max} \simeq 0.10245$ on the wall reaches roughly twice the incident wave amplitude $a_0 = 0.05$ (at $t \simeq 70$). This result is in a good agreement with previous numerical studies on solitary waves interactions[1,3,10] even if the incident shape is not exactly the same. The maximal relative run-up $\mathcal{R}_{\max}/a_0 \simeq 2.34$ is achieved for $\omega_{\max} = 0.145$. The value of $\mathcal{R}_{\max}$ is slowly decreasing for $\omega > \omega_{\max}$.

The dynamics of two waves injected into the domain is similar to the single wave case, but the nonlinear effects become even more apparent (see Figure 1). In a certain range of wave periods ($\omega \in (0.01, 0.05)$), when the second wave impinges on the first reflected wave, a so called dispersive shock wave forms and propagates towards the wall[6,11]. The maximal amplification is achieved when the second wave hits the wall (cfr. last panel of Figure 1), an effect due to nonlinear interactions between two counter-propagating waves:

$$\mathcal{R}_{\max}/a_0 \simeq 3.8, \quad \text{for} \quad \omega = 0.021. \tag{4}$$

High run-up values are possible due to the energy transfer between the first reflected wave and the second incoming wave.

The three regimes (hyperbolic, equilibrium and dispersive) are described on Figure 2, where we show the space-time dynamics of the three-wave system. The left panel shows the hyperbolic regime, on the central panel strong dispersive shocks can be observed, while on the right panel the dynamics is smooth due the dispersion. In the last case the amplification is mainly produced by the linear superposition of the incident and reflected waves. The reflection and interaction are clearly observed by smooth secondary peaks in the space time plots (see Figure 2). Wave interactions described above depend strongly on the frequency
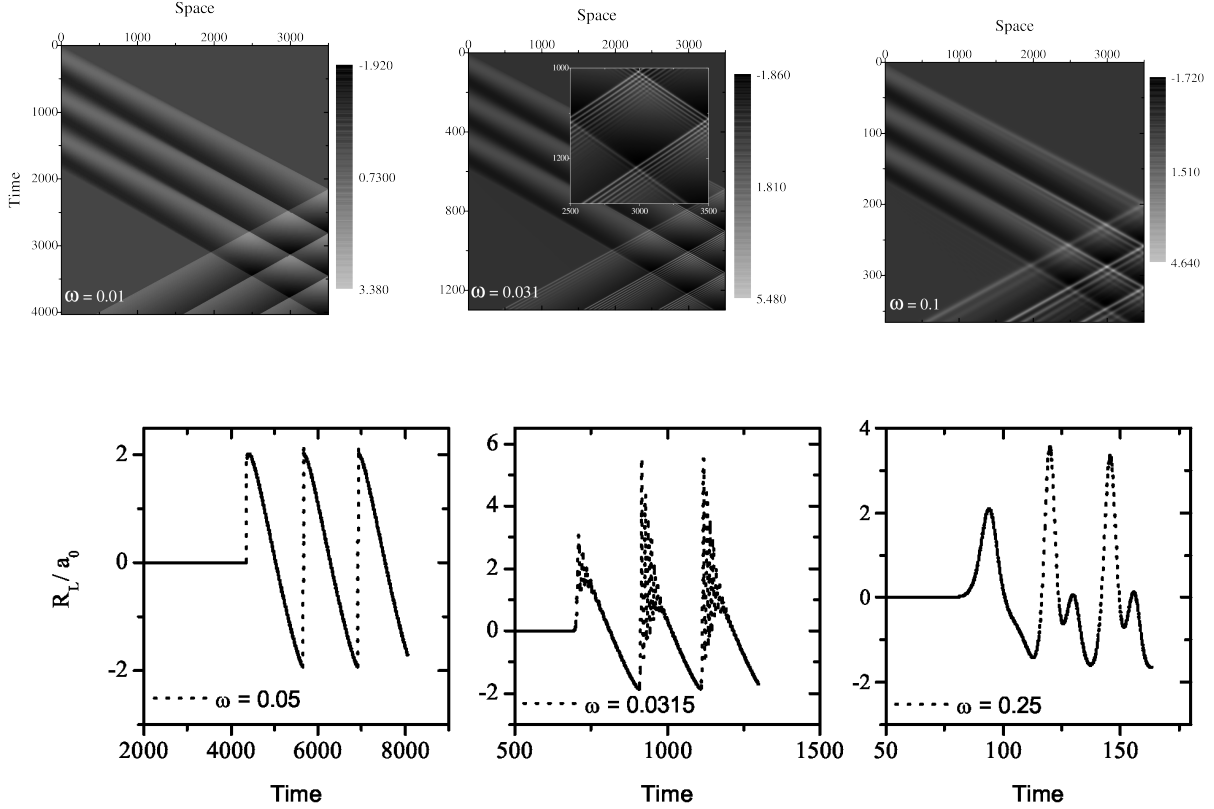
FIG. 2. Upper row space-time evolution plots for three incident waves case shown for three particular values of the wave frequency ω, lower row Time evolution of the wave run-up on the vertical wall for the three incident waves case recorded for several values of the incoming frequency ω. The maximum run-up is achieved for $\omega_{\mathrm{max}} \approx 0.0315$.

ω of the impinging waves. The dependence of the maximal run-up $\mathcal{R}_{\mathrm{max}}$ on the incident wave frequency ω and the number N_w of incident waves is shown on Figure 3, the optimal energy transfer due to dispersive shocks happens for three incident waves. In this case the maximal run-up is observed around $\omega_{\mathrm{max}} = 0.035$ and the amplification is equal to $R_{\mathrm{max}}/a_0 \simeq 5.43$. However, the energy transfer process is saturated for three waves. As the wave frequency increases, the wavelength shortens and the dispersive effects become gradually more important. Around ω_{max} the dispersive effects are balanced with nonlinearities to produce the most pronounced dispersive shock waves. Starting from $\omega \simeq 0.11$ waves become smooth due to dispersive regularization.

More general wave groups have to be studied in future investigations to unveil their potential for focussing on the walls. In addition, we are going to investigate the effect of the forces exerted by incident waves on vertical obstacles, which can be different from the purely kinematic amplitude focussing presented in this study. In other words, it is not clear whether the highest wave will produce the highest dynamic pressure spike on the wall. The effect of the wave amplitude is to be investigated as well since all the processes under consideration are highly nonlinear. Some theoretical explanation of these phenomena is also desireable. However, the difficulty is rather high because of important nonlinearities
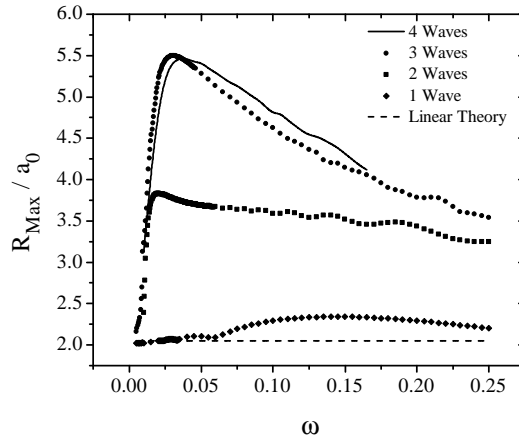
FIG. 3. Maximum wave run-up $\mathcal{R}_{\max}/a_0$ on the right vertical wall as a function of incoming wave frequency for different numbers of incident pulses: 1 (squares), 2 (circles), 3 (triangles) and 4 (solid line). The dashed line represents the linear limit where $\mathcal{R}_{\max}/a_0 \equiv 2$.

mentioned hereinabove. We claim that no linear theory is sufficient to provide a satisfactory explanation of the reported phenomenon.

[1]Chambarel, J., C. Kharif, and J. Touboul, Head-on collision of two solitary waves and residual falling jet formation, *Nonlin. Processes Geophys.*, *16*, 111–122, 2009.

[2]Clamond, D., and D. Dutykh, Practical use of variational principles for modeling water waves, *Physica D: Nonlinear Phenomena*, *241*(1), 25–36, doi:10.1016/j.physd.2011.09.015, 2012.

[3]Cooker, M. J., P. D. Weidman, and D. S. Bale, Reflection of a high-amplitude solitary wave at a vertical wall, *J. Fluid Mech.*, *342*, 141–158, 1997.

[4]Dias, F., and P. Milewski, On the fully-nonlinear shallow-water generalized Serre equations, *Physics Letters A*, *374(8)*, 1049–1053, 2010.

[5]Dutykh, D., D. Clamond, P. Milewski, and D. Mitsotakis, An implicit-explicit finite volume scheme for fully nonlinear Serre equations, *Submitted*, 2011.

[6]El, G. A., R. H. J. Grimshaw, and N. F. Smyth, Unsteady undular bores in fully nonlinear shallow-water theory, *Phys. Fluids*, *18*, 27,104, 2006.

[7]Goda, Y., New wave pressure formulae for composite breakers, in *Proc. 14th Int. Conf. Coastal Eng.*, pp. 1702–1720, 1974.

[8]Green, A. E., and P. M. Naghdi, A derivation of equations for wave propagation in water of variable depth, *J. Fluid Mech.*, *78*, 237–246, 1976.

[9]Nikolkina, I., and I. Didenkulova, Rogue waves in 2006 - 2010, *Nat. Hazards Earth Syst. Sci.*, *11*, 2913–2924, doi:10.5194/nhess-11-2913-2011, 2011.

[10]Pelinovsky, E. N., E. Troshina, V. Golinko, N. Osipenko, and N. Petrukhin, Runup of tsunami waves on a vertical wall in a basin of complex topography, *Phys. Chem. Earth. (B)*, *24*(5), 431–436, 1999.

[11]Wei, G., J. T. Kirby, S. T. Grilli, and R. Subramanya, A fully nonlinear Boussinesq model for surface waves. Part 1. Highly nonlinear unsteady waves, *J. Fluid Mech.*, *294*, 71–92, 1995.

[12]Zheleznyak, M. I., and E. N. Pelinovsky, Physical and mathematical models of the tsunami climbing a beach, in *Tsunami Climbing a Beach*, edited by E. N. Pelinovsky, pp. 8–34, Applied Physics Institute Press, Gorky, 1985.